BRAIN
ORIGINAL ARTICLE

Interictal spikes with and without high-frequency oscillation have different single-neuron correlates

Tim A. Guth,[1,2,3] Lukas Kunz,[1,3,4,5,6] Armin Brandt,[1,3] Matthias Dümpelmann,[1,3] Kerstin A. Klotz,[1,2,3,7] Peter C. Reinacher,[3,8,9] Andreas Schulze-Bonhage,[1,3] Julia Jacobs[2,3,10,11] and Jan Schönberger[1,2,3,7]

See Huberfeld and Le Van Quyen (doi:10.1093/brain/awab349) for a scientific commentary on this article.

Interictal epileptiform discharges (IEDs) are a widely used biomarker in patients with epilepsy but lack specificity. It has been proposed that there are truly epileptogenic and less pathological or even protective IEDs. Recent studies suggest that highly pathological IEDs are characterized by high-frequency oscillations (HFOs). Here, we aimed to dissect these 'HFO-IEDs' at the single-neuron level, hypothesizing that the underlying mechanisms are distinct from 'non-HFO-IEDs'. Analysing hybrid depth electrode recordings from patients with temporal lobe epilepsy, we found that single-unit firing rates were higher in HFO- than in non-HFO-IEDs. HFO-IEDs were characterized by a pronounced pre-peak increase in firing, which coincided with the preferential occurrence of HFOs, whereas in non-HFO-IEDs, there was only a mild pre-peak increase followed by a post-peak suppression. Comparing each unit's firing during HFO-IEDs to its baseline activity, we found many neurons with a significant increase during the HFO component or ascending part, but almost none with a decrease. No such imbalance was observed during non-HFO-IEDs. Finally, comparing each unit's firing directly between HFO- and non-HFO-IEDs, we found that most cells had higher rates during HFO-IEDs and, moreover, identified a distinct subset of neurons with a significant preference for this IED subtype. In summary, our study reveals that HFO- and non-HFO-IEDs have different single-unit correlates. In HFO-IEDs, many neurons are moderately activated, and some participate selectively, suggesting that both types of increased firing contribute to highly pathological IEDs.

1 Epilepsy Center, Medical Center, University of Freiburg, Freiburg, Germany
2 Department of Neuropediatrics and Muscle Disorders, Medical Center, University of Freiburg, Freiburg, Germany
3 Faculty of Medicine, University of Freiburg, Freiburg, Germany
4 Department of Biomedical Engineering, Columbia University, New York, NY, USA
5 Spemann Graduate School of Biology and Medicine (SGBM), University of Freiburg, Freiburg, Germany
6 Faculty of Biology, University of Freiburg, Freiburg, Germany
7 Berta-Ottenstein-Programme, Faculty of Medicine, University of Freiburg, Freiburg, Germany
8 Stereotactic and Functional Neurosurgery, Medical Center—University of Freiburg, Freiburg, Germany
9 Fraunhofer Institute for Laser Technology, Aachen, Germany
10 Department of Paediatrics and Department of Neuroscience, Cumming School of Medicine, University of Calgary, Calgary, Alberta, Canada
11 Hotchkiss Brain Institute and Alberta Children's Hospital Research Institute, University of Calgary, Calgary, Alberta, Canada

Received January 30, 2021. Revised June 07, 2021. Accepted July 06, 2021. Advance access publication August 3, 2021

Correspondence to: Dr Jan Schönberger
Department of Neuropediatrics and Muscle Disorders
Medical Center, University of Freiburg
Mathildenstraße 1, 79106 Freiburg im Breisgau, Germany
E-mail: jan.schoenberger@yahoo.de

Keywords: single unit; interictal spikes; high-frequency oscillations; epilepsy; intracranial EEG
Abbreviations: FR_{norm} = normalized firing rate; HFO = high-frequency oscillation; IED = interictal epileptiform discharge; I_{pref} = preference indicator

Introduction

Interictal epileptiform discharges (IEDs) are brief bursts of paroxysmal activity that are not part of a seizure.[1] They are found in many patients with epilepsy,[2,3] may help to localize epileptogenic foci[4] and possibly reflect disease activity.[2,3] Moreover, IEDs impair learning and memory.[5,6] However, their role in seizure generation has remained controversial. Prior to seizures, some patients have an increase in IEDs, whereas others have stable or even decreased rates.[7] It has also been reported that IEDs are followed by a period of reduced excitability[8] and that their rates decrease after withdrawal of anti-epileptic drugs.[9] IEDs, or at least some of them, might thus also protect against seizures. Several decades ago, the concept of 'red' and 'green' IEDs introduced the idea of two separate IED subtypes with different generation mechanisms and contrary implications for clinical management.[10] But distinguishing truly epileptogenic from less pathological or even protective IEDs has remained a major challenge ever since.

One strategy to identify more pathological IEDs might be to focus on IEDs that carry a high-frequency oscillation ('HFO-IEDs', in contrast to 'non-HFO-IEDs'). HFOs are promising biomarkers of epileptogenicity: resection of HFO-generating areas was associated with seizure-free outcome in several collectives,[11–13] HFO rates increased after reduction of anti-epileptic medication,[14] and HFOs may be involved in seizure generation.[15,16] However, HFOs in general have limited specificity because ripples (80–250 Hz) without co-occurring IED are also generated physiologically, coupled to a low-amplitude 'sharp wave' deflection.[17–20] Recent studies suggest that HFO-IEDs are indeed superior to IEDs and HFOs alone, regarding the delineation of seizure-generating areas,[11,21–23] identification of patients with epilepsy[24] and prediction of seizure risk.[25] Whether HFO-IEDs and non-HFO-IEDs should be categorized as two distinct events, generated by different neuronal networks, is as yet unclear. In rodents, HFO-generating networks have been characterized in great detail, and down to the different contributions of pyramidal cells and various interneuron subtypes.[26–28] Single-unit data from human subjects are rarely available and to date, few studies have examined neuronal firing during IEDs, revealing that a synchronized discharge is followed by a period of sustained inhibition[29] and that firing patterns of cortical neurons are heterogeneous.[30] How different IED subtypes vary in their single-unit composition, and whether particularly epileptogenic IEDs have a distinct signature at the level of individual neurons, has not to our knowledge been examined.

Hence, the purpose of this study was to investigate whether HFO- and non-HFO-IEDs have different single-unit correlates—and if so, to identify mechanisms that are specific to HFO-IEDs. To this end, we analysed hybrid depth electrode recordings from human patients with temporal lobe epilepsy. Our analysis focused on (i) the temporal relationship between IEDs, HFOs and neuronal firing; (ii) single-cell firing in HFO- and non-HFO-IEDs compared to baseline; and (iii) single-cell firing compared directly between HFO- and non-HFO-IEDs.

Materials and methods

Subjects

This study was conducted in patients with medically intractable temporal lobe epilepsy who, as part of their presurgical evaluation, had hybrid depth electrodes[31] (Ad-Tech) implanted into their anterior hippocampus (Fig. 1A; see Supplementary Fig. 1 for representative MRI sections from each patient) using a stereotactic frame (Leksell Frame G, Elekta). We included all subjects treated at the Freiburg Epilepsy Center between March 2018 and June 2019. Two patients had been implanted bilaterally with hybrid depth electrodes; in these, data from both hippocampi were analysed. The study was approved by the Ethics Commission at the University Medical Center Freiburg and written informed consent was obtained from all patients.

Macro- and microelectrode recordings

Stereotactic EEG was recorded with macroelectrode contacts with a sampling rate of 2 kHz using a Neuvo system (Compumedics). Microelectrode recordings were obtained at 30 kHz using a Blackrock NeuroPort system (Blackrock Microsystems). Macro- and microelectrode recordings were aligned in time using trigger pulses sent simultaneously to both recording systems. We thus obtained a maximum temporal shift of <1 ms between macro- and microelectrode recordings. For each patient, a seizure-free 30-min segment of slow-wave sleep was selected. Further analysis was performed using custom-written MATLAB (2015b and 2018b, MathWorks, Natick, MA) scripts.

Detection of IEDs and HFOs

IEDs and HFOs were analysed in a bipolar recording montage from the two most distal macroelectrode contacts (Fig. 1B). Events were identified visually using the Harmonie Viewer software (Stellate, Montreal, QC, Canada). IEDs were identified at a temporal resolution of 10 s per screen. We only marked spikes and sharp waves without their corresponding slow wave. HFOs were identified based on previously established procedures.[14] In brief, we split the screen vertically and displayed filtered traces (finite impulse response filter, order 63) at maximum temporal resolution (0.4 s on each half). Ripples (80–250 Hz) and fast ripples (>250 Hz) associated with IEDs were marked simultaneously on the two halves of the split screen. An event had to consist of at least four oscillatory cycles to be considered an HFO. Events associated with artificial sharp transients were excluded meticulously. IEDs with a co-

occurring HFO were defined as 'HFO-IEDs', while those without an HFO were called 'non-HFO-IEDs'. To examine inter-rater reliability, a second reviewer also identified HFOs in randomly selected 3-min intervals, blinded to the first reviewer's detections. Cohen's kappa coefficient was 0.75 and thus higher than described in a previous study.[32] For additional analyses, automated detection was performed using the Delphos algorithm[33,34] (see Supplementary material for a detailed description).

Single-unit analysis

Microelectrode recordings were obtained from eight of the wires in each hybrid electrode, with the ninth electrode used as a reference microwire. Single- and multi-unit activity were extracted using the spike sorting algorithm Wave_clus[35] (Fig. 1C). Here, the term 'spike' refers to single-unit action potentials, and not to IEDs. Spike detection was performed on a band-pass (300 Hz–3 kHz) filtered signal. Single units were identified based on the following previously established criteria[36]: (i) spike shape and its variance; (ii) ratio between peak of the mean waveform (i.e. spike amplitude) and standard deviation at the first sampling point (i.e. noise) >3; (iii) inter-spike interval distribution; and (iv) $<1\%$ of the spikes with an inter-spike interval <3 ms, which takes into account that neurons have a refractory period (see Supplementary Fig. 2 for quality metrics[37]). Spike clusters that did not fulfil these criteria were only considered for multi-unit analyses. Putative pyramidal cells and interneurons were distinguished based on procedures described in previous studies: For each single unit, we first calculated the parameters firing rate, spike symmetry and mean of the autocorrelation function.[38] A k-means algorithm was then applied on the normalized parameters to cluster our single units into two groups of putative cell types.[39]

Statistical analysis

In general, statistical hypothesis testing was conducted using two-tailed non-parametric tests. A significance level of 5% was chosen. Moreover, we performed surrogate data analyses to address additional questions, which are described in detail below.

To identify periods of significantly altered multi-unit activity during the course of IEDs, we performed cluster-based surrogate statistics.[40,41] First, firing rates were compared to baseline activity: To this end, we calculated each unit's firing rate for bins of 20 ms and then conducted two-tailed paired *t*-tests against baseline, i.e. the firing rate during all segments not marked as IEDs. Clusters of contiguous increased or decreased bins ($P < 0.05$) were extracted and the sum of *t*-values was calculated for each of these clusters ('empirical summary *t*-values'). Next, we randomly flipped each unit's firing rate time course over its baseline with a 50% chance[42] and identified the clusters with maximum and minimum sum of *t*-values ('surrogate summary *t*-value'). This step was repeated 5000 times to obtain a distribution of surrogate summary *t*-values. Multi-unit activity was considered significantly altered during a cluster if its empirical summary *t*-value ranked $>97.5\%$ of all positive surrogate summary *t*-values or $<2.5\%$ of all negative surrogate summary *t*-values. In a second analysis, we directly compared the time course of multi-unit activity between HFO- and non-HFO-IEDs. Here, surrogate datasets were created by randomly permuting the group labels 'HFO-IED' and 'non-HFO-IED' between firing rate time courses.

To examine whether a unit's firing rate was significantly altered during IEDs (Supplementary Fig. 3A), we first computed its normalized firing rate FR_{norm} ('empirical FR_{norm}')

$$FR_{norm} = \frac{FR_{IED}}{FR_{baseline}} \quad (1)$$

where FR_{IED} is its firing rate during IEDs and $FR_{baseline}$ is its firing

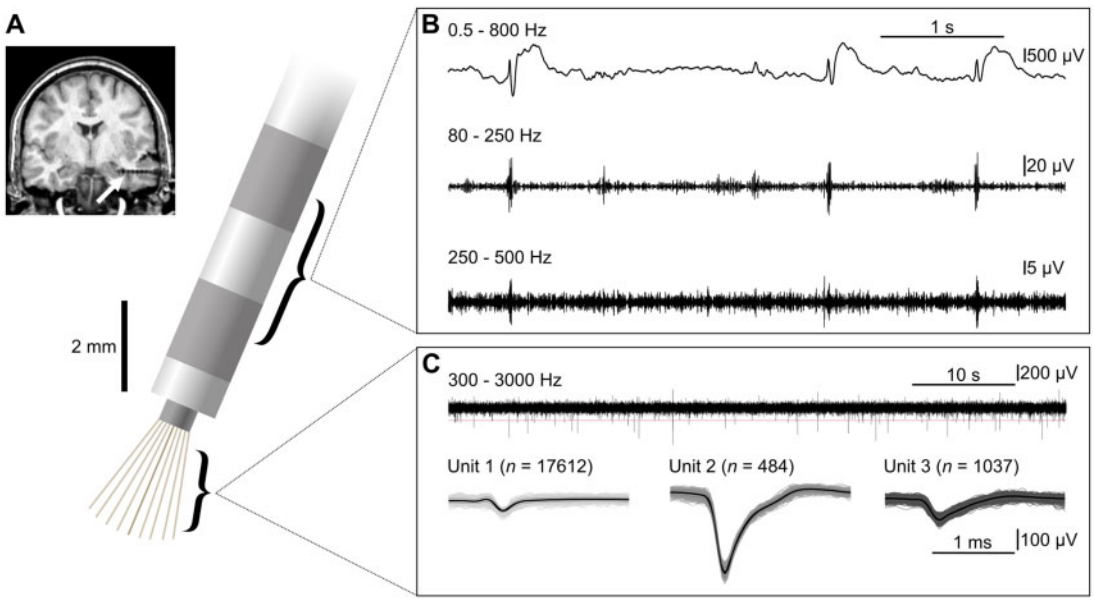

Figure 1 Our approach: IEDs and HFOs were recorded with clinical macroelectrodes, single units were recorded with microwires. (**A**) Schematic of a hybrid depth electrode. *Top left*: Post-implantation MRI. Arrow indicates hybrid depth electrode implanted into the anterior hippocampus. (**B**) Bipolar stereotactic EEG recording from the two most distal macroelectrode contacts. IEDs were identified in the wideband-filtered signal (*top*), HFOs in band-pass filtered traces [ripples: 80–250 Hz (*middle*), fast ripples: 250–500 Hz (*bottom*)]. (**C**) Microelectrode recordings and identification of single units. *Top*: Sixty seconds of microwire data. Horizontal line indicates the threshold used for spike detection. *Bottom*: Spike shapes of the three units extracted from this wire. The *left* unit was classified as a multi-unit, the *middle* and *right* units were classified as single units.

rate during all segments that had not been marked as IEDs. Next, we shifted the unit's spike train circularly by a random time interval <30 min (with the end of the session wrapped to the beginning) and again computed FR_{norm} ('surrogate FR_{norm}'). This step was repeated 5000 times to compute a distribution of surrogate FR_{norm}. A unit's firing rate was considered significantly altered if its empirical FR_{norm} ranked >97.5% or <2.5% of all surrogate FR_{norm}. Finally, a two-sided binomial test was used to examine whether the number of significantly increased or decreased units was greater than expected by chance.

To examine if a unit's firing rate differed significantly between HFO-IEDs and non-HFO-IEDs (Supplementary Fig. 3B), we performed another permutation test.[40] First, we calculated a preference indicator I_{pref} ('empirical I_{pref}').

$$I_{pref} = \frac{FR_{HFO-IED} - FR_{non-HFO-IED}}{FR_{HFO-IED} + FR_{non-HFO-IED}} \quad (2)$$

Next, we randomly shuffled the labels of all detected IEDs and again computed I_{pref} ('surrogate I_{pref}'). This step was repeated 5000 times to compute a distribution of surrogate I_{pref}. A unit's firing rate was considered significantly different between HFO- and non-HFO-IEDs if its empirical I_{pref} ranked >97.5% or <2.5% of all surrogate I_{pref}. Again, a two-sided binomial test was performed to examine whether the number of significantly altered single units was greater than expected by chance. Moreover, the median empirical I_{pref} (of all units) was compared to the distribution of median surrogate $I_{pref,}$ computed based on each of the permutations described above, to examine whether this parameter differed significantly from chance.

Data availability

Data supporting the findings of this study are available within the article and the Supplementary material. Upon reasonable request, additional data can be provided by the corresponding author.

Results

Patients and basic characteristics of IEDs and HFOs

Nine patients with drug-resistant temporal lobe epilepsy (six females, three males; age: median 28 years, range 24–52 years; see Table 1 for more clinical data) of various aetiologies were included. Eight of them had a seizure onset zone involving the hippocampus; in the remaining individual, seizures originated from the temporal pole. All patients had clearly visible IEDs with and without HFOs in their macroelectrode recordings from the anterior hippocampus. In total, 6507 IEDs were identified, of which 63.4% were associated with HFOs ('HFO-IEDs'; Fig. 2A) and 36.6% were not ('non-HFO-IEDs'; Fig. 2B). Ninety-one per cent of the HFO-IEDs co-occurred with at least one ripple and 44.0% carried at least one fast ripple.

To provide evidence that HFO-IEDs reflect epileptogenic activity, we conducted additional analyses based on automated detection (Supplementary material), which showed that HFO-IED rate and percentage were significantly higher in seizure-onset zone than in non-seizure-onset zone channels (Supplementary Fig. 4). Moreover, the percentage of HFO-IEDs increased prior to seizures and HFO-IEDs were more often associated with IED propagation (Supplementary Fig. 5 and Supplementary material).

Coupling of HFOs to the ascending phase of IEDs

First, we investigated whether HFOs are temporally coupled to a distinct part of IEDs (Fig. 2C). Referenced to the peak of the IEDs,

Table 1 Patient characteristics

Patient ID/ Sex/Age, years	Epilepsy diagnosis/ Hemisphere	MRI/Pathology	Seizure onset zone	Surgery/Outcome (Engel class)	AEDs	Multi units/Single units/Hemisphere
1/M/27	TLE/L	Meningoencephalocele T pole L, S/p T pole resection L (outcome Engel IIIB)	T lateral L, possibly also Hc L	ATL L/IA	LTG, BRV	10/4/L
2/F/33	TLE/B	Sphenoid wing dysplasia L with prolapse of the L T lobe, gangliolioma straight gyrus L	Hc + amygdala L, straight gyrus L, Hc R	EL L frontal/IVB	OXC, BRV, CLB	7/4/R
3/F/23	TLE/R	FCD T pole R, T_2 hyperintensity amygdala R	Hc + amygdala R, T pole R	–	LEV	8/0/R
4/F/26	TLE/L	Hc malrotation L, prominent L amygdala	Hc L, mesial T pole L	–	BRV, PER	12/5/L
5/F/23	TLE/R	HS R	Hc R, possibly also T pole R	T pole resection + AH R/IA	BRV, LCS	11/0/R
6/F/43	TLE/B	Meningoencephaloceles T pole B	T pole L, subclinical seizures from T pole R	T pole resection L/IA	ESL, ZNS	8/1/L 5/3/R
7/F/51	TLE/R	No epileptogenic lesion	Hc R, T lateral R, central operculum R	–	OXC, LEV	16/9/R
8/M/48	TLE/R	Hc gliosis R	Hc + amygdala R	AH R/IA	BRV, LCS, PER	10/3/L 9/3/R
9/M/28	TLE/R	FCD T pole R	Mesial T pole R, Hc R	T pole resection + AH R/IB	OXC	12/8/R

AEDs = anti-epileptic drugs; AH = amygdalohippocampectomy; ATL = anterior temporal lobectomy; B = bilateral; BRV = brivaracetam; CLB = clobazam; F = female; EL = extended lesionectomy; ESL = eslicarbazepine acetate; FCD = focal cortical dysplasia; Hc = hippocampus; HS = hippocampal sclerosis; L = left; LCS = lacosamide; LEV = levetiracetam; LTG = lamotrigine; M = male; OXC = oxcarbazepine; PER = perampanel; R = right; s/p = status post; T = temporal; TLE = temporal lobe epilepsy; ZNS = zonisamide

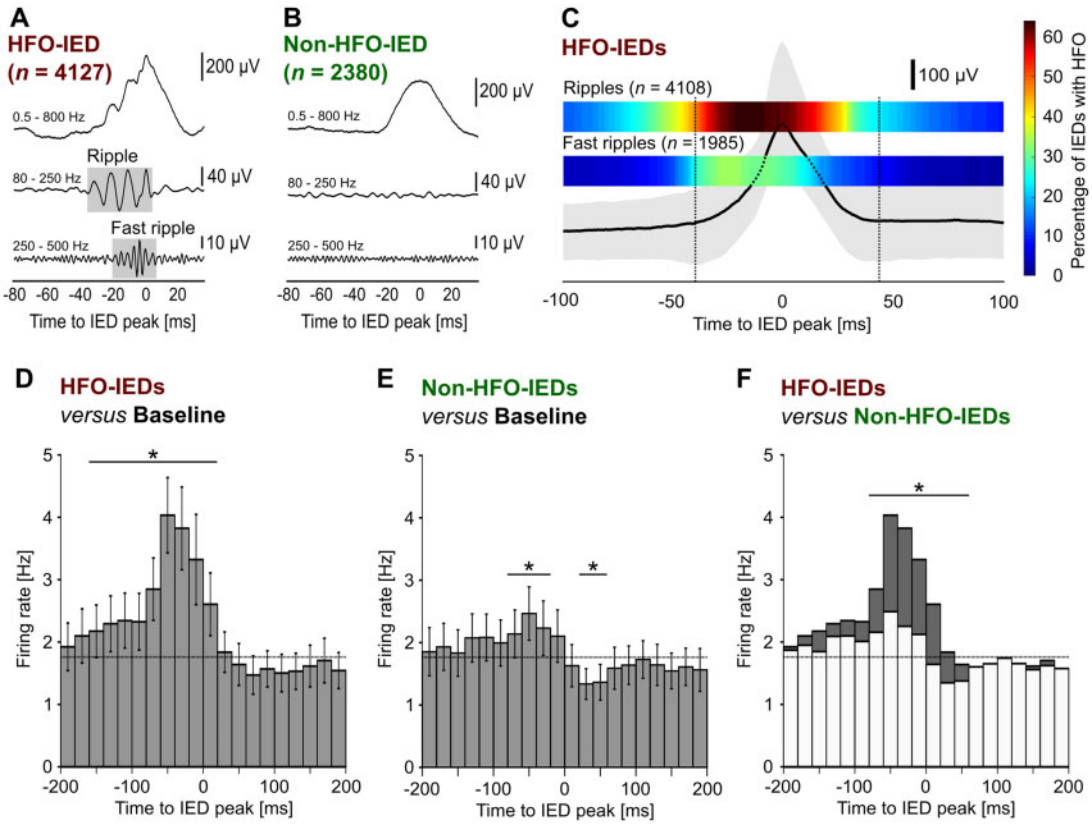

Figure 2 HFOs and neuronal firing are coupled to the ascending phase of IEDs. (**A**) Example IED with associated HFO (HFO-IED). Boxes in grey indicate a visually identified ripple (80–250 Hz) and a fast ripple (250–500 Hz) in band-pass filtered traces. (**B**) Example IED without associated HFO (non-HFO-IED). (**C**) Temporal coupling of IEDs and HFOs. Median (bold line) and 25th to 75th percentile (grey-shaded area) of all HFO-IEDs; the two heat maps above show the percentage of IEDs with a ripple or fast ripple at a specific time relative to the IED peak. Note that HFOs occur preferentially during the ascending phase of IEDs. (**D**) Temporal coupling of HFO-IEDs and multi-unit activity ($n = 108$ units). Histogram shows mean firing rate and standard error of the mean (error bars) during HFO-IEDs. Asterisks indicate significant changes compared to baseline (horizontal bar, $P < 0.001$). Note that a pronounced increase in multi-unit activity occurs before and during the IED peak. (**E**) In non-HFO-IEDs, there was only a moderate pre-peak increase ($P < 0.01$), followed by a post-peak suppression ($P < 0.05$) of firing. (**F**) Direct comparison of HFO- versus non-HFO-IEDs reveals significantly higher firing in HFO-IEDs from –80 to +60 ms ($P < 0.001$).

the median ripple occurred from –42 ms until +22 ms. Fast ripples started on average at –25 ms and ended at –1 ms. The highest proportion of IEDs carrying an HFO was found at –13 ms for ripples and at –27 ms for fast ripples. On average, 62.7% of each ripple and 61.5% of each fast ripple occurred before the IED peak, which in both cases was significantly different from the 50% expected by chance ($P < 0.001$, Wilcoxon signed-ranks test). In summary, these findings suggest that both ripples and fast ripples occur preferentially during the ascending phase of HFO-IEDs.

Coupling of neuronal firing to the ascending phase of IEDs

Hypothesizing that coupling of HFOs to IED phase is accompanied by an increase in neuronal firing, we characterized the temporal course of multi-unit activity during IEDs. Firing rates were higher during the ascending than during the descending phase of IEDs, both for HFO-IEDs ($P < 0.001$, Wilcoxon signed-ranks test, $n = 108$ units) and non-HFO-IEDs ($P < 0.001$). Cluster-based surrogate testing was then performed to identify periods of significantly altered multi-unit activity (see the 'Materials and methods' section). For HFO-IEDs, there was a pronounced increase from baseline before the peak of the IED, which was significant from –160 to +20 ms ($P < 0.001$, cluster-based surrogate test; Fig. 2D). This increase was found in both ripple- and fast ripple-IEDs (Supplementary Fig. 6). In non-HFO-IEDs, there was only a moderate pre-peak increase (from –60 to –20 ms; $P < 0.01$), and, moreover, a post-peak suppression of neuronal firing, which was significant from +20 to +60 ms ($P < 0.05$). Next, we compared multi-unit activity directly between HFO- and non-HFO-IEDs and found significantly higher firing in HFO-IEDs from –80 ms to +60 ms ($P < 0.001$, cluster-based permutation test). Additional analyses revealed that neuronal firing in IED-ripples was significantly higher than in ripples without clearly visible IED (Supplementary Fig. 7). In summary, these data suggest that especially in HFO-IEDs, there is an increase in neuronal network activity, with onset clearly before the peak of the IED.

Single-unit firing during HFO- and non-HFO-IEDs: comparison to baseline

Next, we aimed to characterize the behaviour of individual neurons during HFO- and non-HFO-IEDs. Forty of our units were classified as single units (see Supplementary Fig. 2 for details on quality metrics). Of these, 35 were classified as putative pyramidal cells and five as putative interneurons (Fig. 3A). We found that single-unit firing rate was significantly higher during HFO-IEDs than during non-HFO-IEDs ($P < 0.05$, Wilcoxon signed-ranks test; Fig. 3B). For each single unit, we also determined a normalized firing rate (FR_{norm}), which compares a unit's firing during IEDs to its baseline firing rate. Ranking our single units according to FR_{norm},

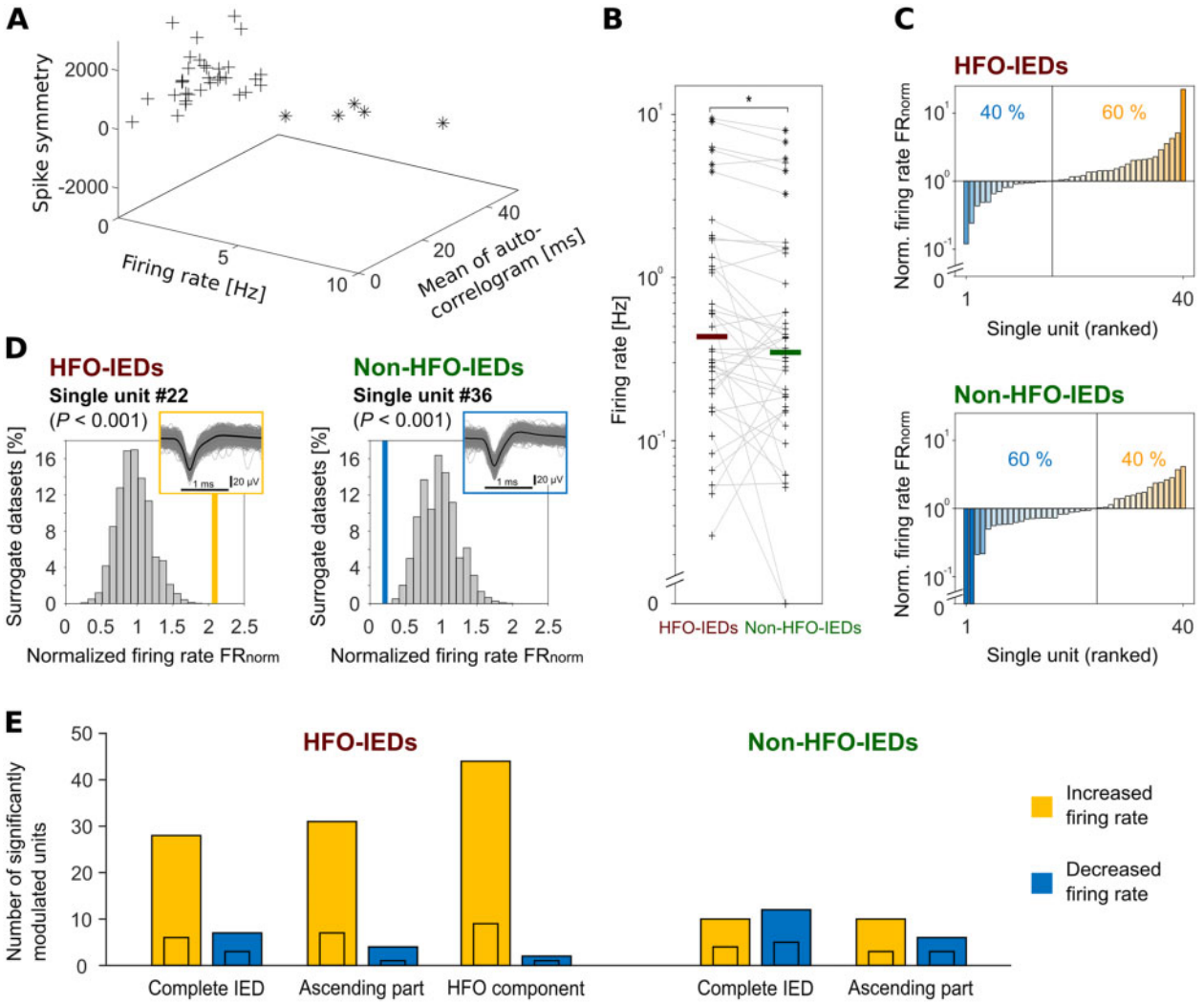

Figure 3 Comparison to baseline: single-unit firing increases during HFO-IEDs. (**A**) Distinction of neuronal subtypes. Applying a k-means algorithm, we classified 35 single units as putative pyramidal cells (plus signs) and five as putative interneurons (asterisks). (**B**) Single-unit firing rates are significantly higher during HFO-IEDs than during non-HFO-IEDs ($P < 0.05$). Each plus sign represents one putative pyramidal cell; asterisks represent interneurons. Grey lines connect each single unit's firing rate during HFO- and non-HFO-IEDs to facilitate comparison. Bold horizontal lines indicate median firing rates. Values > 0 are plotted on a logarithmic scale, the y-axis is broken to show single units that did not fire at all. (**C**) Single-unit firing during HFO-IEDs (*top*) and non-HFO-IEDs (*bottom*), comparison to baseline firing rates. Single units are ranked in ascending order according to their normalized firing rate FR_{norm}. The vertical line separates single units firing below baseline from those firing above baseline. During HFO-IEDs, 40% fired below baseline and 60% above. During non-HFO-IEDs, 60% fired below baseline and only 40% above. (**D**) Two example single units. *Left*: Unit #22 with significantly increased firing ($P < 0.001$) during HFO-IEDs. *Right*: Unit #36 with significantly decreased firing ($P < 0.001$) during non-HFO-IEDs. To identify such units, we compared each unit's FR_{norm} ('empirical FR_{norm}', bold orange and blue vertical lines) to a distribution of surrogate FR_{norm} (histogram). *Insets*: Mean (bold black line) and individual (grey lines) spike shapes. (**E**) Summary of units with significantly altered firing during different parts of HFO- and non-HFO-IEDs. Note that many units increased firing specifically during the HFO component (44 units, only two decreased) or ascending phase (31 units, only four decreased) of HFO-IEDs ($P < 0.001$). The numbers of significantly increased and decreased units were different between HFO- and non-HFO-IEDs ($P < 0.05$, $n = 108$ units). Small *inset* bars indicate numbers of single units.

we found that single units behaved differently during HFO- and non-HFO-IEDs ($P < 0.05$, two-sample Kolmogorov-Smirnov test): during HFO-IEDs, 60% of the single units had higher firing rates than at baseline and 40% fired less (Fig. 3C). In contrast, during non-HFO-IEDs, only 40% increased their firing rate and 60% were suppressed. Similar results were obtained as we performed this analysis on all our units (Supplementary Table 1).

Comparison to baseline II: units with significantly altered firing

To identify neurons with significantly altered firing during HFO- or non-HFO-IEDs, we then performed surrogate data analyses (Fig. 3D; see the 'Materials and methods' section and Supplementary Fig. 3A). During HFO-IEDs, 28 units with a significant increase in firing were found (26%; $P < 0.001$, binomial test; six of them single units; Fig. 3E and Supplementary Figs 8A and 9A), compared to seven with a decrease (6%; three single units). This trend of identifying more units with significantly increased firing became more obvious when we focused on the HFO component; here, we identified 44 such units (41%; $P < 0.001$; nine single units), compared to only two with a decrease (2%, one single unit). A similar finding was obtained for the ascending part of HFO-IEDs [31 units increased (29%; $P < 0.001$; seven single units), four units decreased (4%, one single unit)]. During non-HFO-IEDs, in contrast, there was no clear imbalance between positively and negatively

modulated neurons [10 units increased (9%; four single units), 12 decreased (11%; five single units)], which was significantly different from HFO-IEDs ($P < 0.05$, Fisher's exact test; $n = 108$ units). Focusing on the ascending phase of non-HFO-IEDs did not yield substantially different results. There was no obvious difference between putative pyramidal cells and interneurons regarding their involvement in HFO- and non-HFO-IEDs. In a control analysis, we found that increased firing did not alter spike shapes systematically, which excludes a major confounding effect on spike sorting (see the Supplementary material for details). In summary, these data not only underline that HFO-IEDs are associated with increased neuronal firing—they moreover demonstrate that we can identify participators at the level of individual cells.

Single unit firing in HFO-IEDs versus non-HFO-IEDs

Finally, we aimed to investigate whether there are neurons that are specifically associated with one IED subtype, i.e. with either HFO-IEDs or non-HFO-IEDs. To this end, we computed a preference indicator I_{pref} for each single unit, which quantifies to what extent that unit fired more during HFO- or non-HFO-IEDs [Fig. 4A(i) and Supplementary Fig. 10]. At the network level, two possible mechanisms could be hypothesized, which would both result in higher average firing rates during HFO- than during non-HFO-IEDs [Fig. 4A(ii)]: there might be a mild, rather unspecific increase across the whole network (hypothesis 1) or only some neurons might specifically increase firing during HFO-IEDs, but not during non-HFO-IEDs (hypothesis 2). Of note, these two hypotheses are not mutually exclusive.

Ranking our single units according to their I_{pref}, we observed that 65% had an $I_{pref} > 0$, i.e. they were more active during HFO-IEDs than during non-HFO-IEDs (Fig. 4B). A similar result was obtained when we performed this analysis on all our units (71% with $I_{pref} > 0$; Supplementary Table 2). Many single units had a moderate preference for HFO-IEDs, as reflected by a median I_{pref} of 0.12 ($P < 0.01$, permutation test). These findings support hypothesis 1. On the other hand, some single units also had a clearly higher I_{pref} of ~0.5 or almost 1, meaning that their firing rate during HFO-IEDs was three or more times higher than during non-HFO-IEDs. We thus also conducted a permutation test to examine for each unit whether its firing rate differed significantly between HFO- and non-HFO-IEDs (Fig. 4C; see the 'Materials and methods' section and Supplementary Fig. 3B). Thirty-nine such units (eight single units) were found, of which 30 (28% of all units; six single

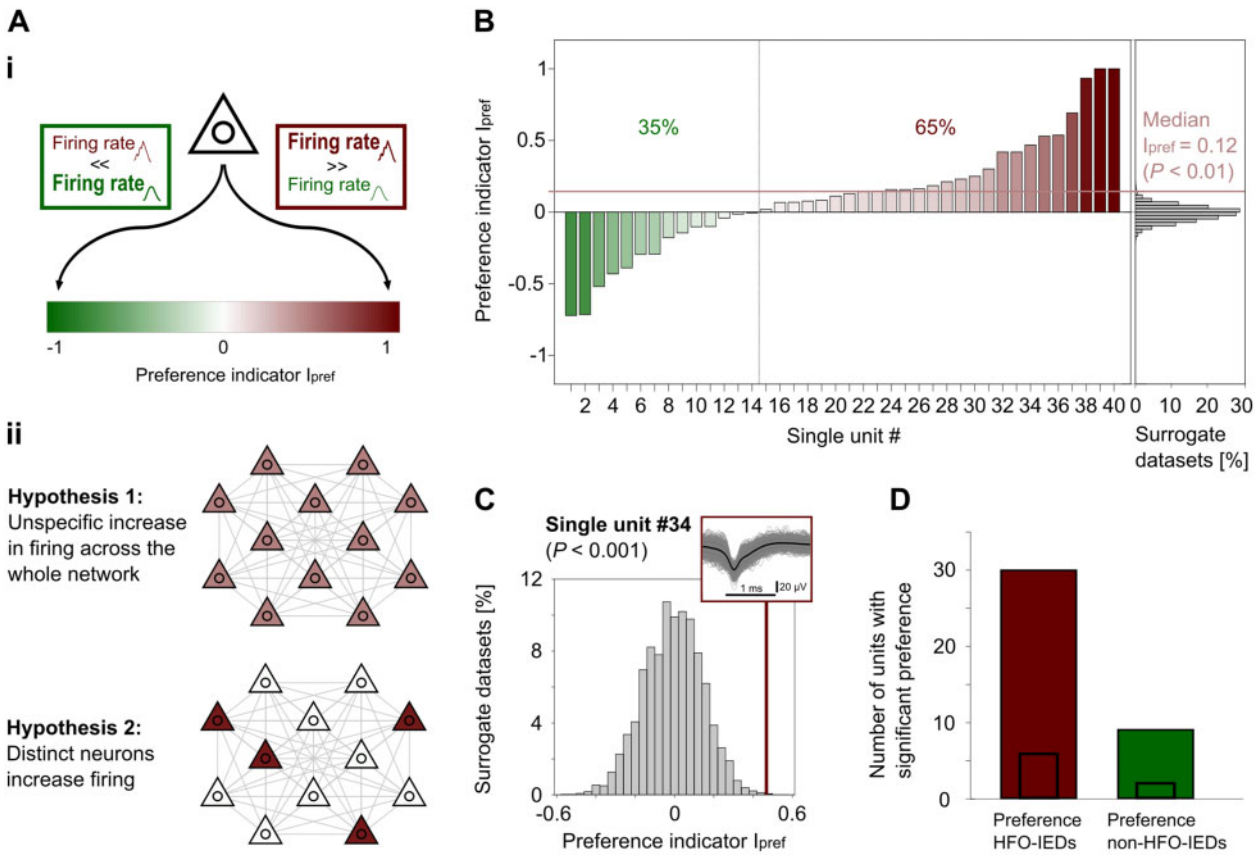

Figure 4 Comparison HFO-IEDs versus non-HFO-IEDs: evidence for two complementary mechanisms. [**A(i)**] For each single unit, we calculated a preference indicator I_{pref}, which quantifies to what extent that unit fired more during HFO-IEDs (I_{pref} almost 1, red) or more during non-HFO-IEDs (I_{pref} almost –1, green). [**A(ii)**] Two hypotheses on neuronal firing in HFO- versus non-HFO-IEDs. Hypothesis 1: The presence of an HFO on IEDs is accompanied by a mild, rather unspecific increase in firing across the whole network. Hypothesis 2: Only some neurons specifically increase firing during HFO-IEDs, but not during non-HFO-IEDs. (**B**) Comparison of single-unit firing during HFO-IEDs to firing during non-HFO-IEDs. Single units are ranked according to their I_{pref} (*left*). The vertical line separates single units firing more during non-HFO-IEDs (35%) from those firing more during HFO-IEDs (65%). Red horizontal line indicates median I_{pref}, which was higher than expected by chance ($P < 0.01$). Distribution of surrogate median I_{pref} (histogram) is shown for comparison (*right*). (**C**) Example single unit (#34) with preferential firing during HFO-IEDs. A comparison of this unit's I_{pref} ('empirical I_{pref}', bold red vertical line) to the distribution of surrogate I_{pref} (histogram) reveals that this unit fired significantly more during HFO-IEDs than during non-HFO-IEDs ($P < 0.001$). *Inset*: Mean (bold black line) and individual (grey lines) spike shapes of this unit. (**D**) Summary of units with significantly different firing between HFO- and non-HFO-IEDs. Note that of 39 such units (from $n = 108$ units in total), 30 had a significant preference for HFO-IEDs ($P < 0.001$). Small *inset* bars indicate numbers of single units.

units) fired significantly more during HFO-IEDs ($P < 0.001$, binomial test; Fig. 4D and Supplementary Figs 8B and 9B), suggesting that they were specifically associated with HFO-IEDs rather than non-HFO-IEDs. Thus, we also provide evidence for hypothesis 2. Again, no obvious differences were observed between putative pyramidal cells and interneurons. It can be concluded that our data provide evidence for both hypothesized mechanisms—and that these mechanisms might act in a complementary fashion.

Discussion

This study shows that 'HFO-IEDs' and 'non-HFO-IEDs' are different at the single-unit level. We report that HFOs and neuronal firing are coupled to the ascending phase of IEDs and identified several single units with significantly increased firing during the HFO component and ascending phase of HFO-IEDs. During non-HFO-IEDs, in contrast, single-unit activity was similar to baseline and frequently even decreased. Moreover, we provide evidence for two complementary mechanisms underlying increased firing during HFO-IEDs: our data suggest that there is both a mild increase across the whole network and a pronounced increase in some, selectively participating neurons. We discuss various aspects of these key findings below.

Coupling of HFOs and neuronal firing to ascending phase of IEDs

Our data suggest that ripples and fast ripples occur preferentially during the ascending phase of IEDs. This finding is in line with previous reports on fast oscillations preceding IEDs.[23,43–45] Moreover, we observed an increase in neuronal firing before the peak of the IED, which was significantly higher in HFO-IEDs. This increase was found in both ripple- and fast ripple-IEDs. It could be hypothesized that HFO-IEDs are generated close to the recording site, whereas non-HFO-IEDs mainly reflect propagated events. If this were true, recording HFO-IEDs with increased firing would indicate that the electrode was located at or near to an epileptic generator, which would be useful information for clinical evaluation. Our data clearly suggest that HFOs and an increase in firing contribute to the generation of at least many IEDs. Such a concept would be compatible with the proposed mechanism of a paroxysmal depolarizing shift, which involves bursts of action potentials at up to ~400 Hz.[46–48] To verify the impact of this mechanism in patients with epilepsy, however, more detailed analyses of single-unit firing sequences will be indispensable.

Different single-unit behaviour in HFO- and non-HFO-IEDs

It can be concluded from our results that HFOs and increased neuronal firing are involved in the generation of many IEDs, those that we call 'HFO-IEDs'. A second line of evidence supporting this concept comes from the single-unit analyses we performed. The majority of our units fired above baseline during HFO-IEDs and, even more noteworthy, approximately one-third increased firing significantly during the HFO component or ascending part of HFO-IEDs. It may be tempting to speculate that some of these cells could be 'hub cells' found in animal and model studies,[49,50] but at least there seem to be neurons that participate with some consistency in a distinct type of network event, in our case HFO-IEDs. In non-HFO-IEDs, in contrast, the majority of single units fired below baseline. A concept synthesizing these results would be that HFO-IEDs are a distinct subtype of IEDs, characterized by increased firing—which is facilitated by rhythmic inhibition that orchestrates local hypersynchrony for ripples[26,51] and sequential activation of small clusters for fast ripples.[52,53] From a mechanistic perspective, it thus seems plausible that HFO-IEDs are closely linked to epileptogenicity, and that they could be a better biomarker than IEDs or HFOs alone, as recent studies suggest.[11,21,22,25]

Categorizing IEDs based on their association with HFOs: a reasonable approach?

Several decades ago, it was hypothesized that there are multiple types of IEDs and that different types may have different implications for clinical management.[10] More recent studies have underlined such variability, showing for example that no more than ~30% of the significantly modulated cells participate in individual IEDs[30] and that network events in a rodent model of epilepsy are generated by variable combinations of several small assemblies.[54,55] So, is it appropriate to categorize IEDs and to classify them into only two groups? We followed such an approach because recent clinical studies suggested that IEDs with HFOs form a distinct class—and our data support this view because we identified single-unit behaviour that is specific to HFO-IEDs and not found in non-HFO-IEDs. One last finding illustrating this concept is that approximately one-third of our units had a significant preference for either HFO- or non-HFO-IEDs, i.e. they selectively adapted their firing rate according to whether or not an IED carried an HFO. This indicates a specific involvement in one of the two network events. A major conclusion from our study therefore is that HFO- and non-HFO-IEDs have clearly different single-unit correlates, or 'fingerprints', which supports the concept of categorizing IEDs based on their association with HFOs.

HFO-IEDs and physiological sharp wave-ripples

Ripple oscillations also occur physiologically. An extensive body of evidence suggests that they play an important role in memory consolidation. Especially in rodent hippocampi, such physiological ripples often occur coupled to a sharp wave.[17,18,20] Given that these 'sharp wave-ripple' complexes are also associated with increased neuronal firing,[17,19] it cannot be excluded that some HFO-IEDs might not reflect epileptic, but merely physiological activity. However, several lines of evidence suggest that the majority of our HFO-IEDs do not correspond to typical sharp wave-ripples: (i) we identified IEDs as done by clinical epileptologists, with amplitudes of ~5–10 times higher than physiological sharp waves[56]; (ii) the increase in multi-unit firing during IED-ripples was significantly higher than in ripples without clearly visible IED; and (iii) additional analyses in our patients confirmed that HFO-IEDs were specifically associated with epileptic activity. This does not exclude that HFO-IEDs and physiological sharp wave-ripples are based on similar mechanisms. In fact, our findings would be consistent with the concept that epilepsy exploits the neuronal machinery underlying physiological sharp wave-ripples to generate HFO-IEDs.[20]

Distance between macroelectrodes and microwires

We analysed IEDs and HFOs in macroelectrode recordings because those are widely used for clinical investigation. Besides, key prior studies on the diagnostic value of these biomarkers have also been based on macroelectrode data. But it is not trivial to disentangle interactions between IEDs and HFOs because IEDs often spread across large brain volumes, whereas HFOs are typically generated by smaller neuronal networks.[57,58] Moreover, as single-unit activity is correlated to these macroelectrode IEDs and HFOs, the spatial distance between microwires and macroelectrode contacts should be considered. This distance may *in situ* be negligible for some

of our wires, but up to several millimetres for others. Macroelectrodes probably detect activity up to a few millimetres from their tip,[59] whereas microwires only 'see' action potentials within a radius of ~100 μm.[60,61] With this in mind, it seems noteworthy that many of our units were significantly modulated by the analysed macroelectrode events—and that we found clear differences between HFO- and non-HFO-IEDs. Our study thus complements previous work on IEDs from microelectrodes.[29,30,43] It can be concluded that combined macro- and microelectrode recordings are a powerful tool, enabling us to dissect EEG patterns known from clinical practice at the single-unit level.

Limitations and outlook

This study is limited in several ways, and additional work is needed to further investigate the mechanisms underlying IEDs at the single-cell level. We focused on temporal lobe epilepsy and the anterior hippocampus to obtain a fairly homogeneous dataset. Such a study may have model character, but one should remain cautious about generalizing to other brain regions. Single-unit identification was performed based on strict criteria, but at the cost of being left with a lower number of unequivocal single units. We were able to reproduce our findings in a complementary analysis of all our units. With regard to possible differences between pyramidal cells and interneurons, however, we propose that a larger sample be examined before we draw a conclusion. Further studies will be required to dissect how individual cells are temporally coupled to HFOs, and whether they form reoccurring assemblies, or rearrange in a more chaotic fashion. Such questions have already been addressed in animal models,[26,52,55] but clearly require further investigation in human patients. Finally, a specific increase in HFO-IEDs prior to seizures has to our knowledge only been reported once.[62] An interesting aim of future studies could be to demonstrate that only a distinct subgroup of IEDs (e.g. those with an HFO or a specific single-unit 'fingerprint') systematically reoccurs during the transition to seizures or impairs cognition. Such evidence would confirm a direct link between such network activity and disease burden, possibly opening a door for clinical application.

Conclusion

This study shows that HFO- and non-HFO-IEDs are different at the single-unit level. In HFO-IEDs, many neurons are moderately activated, and some participate selectively. It can be concluded that these two variants of increased firing contribute to the generation of a highly pathological subtype of IEDs.

Acknowledgements

The authors thank all the patients that participated in this study and the nursing and physician staff at the Freiburg Epilepsy Center.

Funding

J.J. was supported by the German Research Foundation (DFG; JA 1725/4-1). K.A.K. and J.S. were supported by the Berta-Ottenstein-Programme, Faculty of Medicine, University of Freiburg. L.K. was supported by the German Research Foundation (DFG; KU 4060/1-1), the Federal Ministry of Education and Research (BMBF; 01GQ1705A), by National Science Foundation (NSF) grant BCS-1724243, and by NIH/NINDS grant U01 NS113198-01. P.C.R. has received research support from the Fraunhofer Society and personal fees, travel support and honoraria from Boston Scientific, Brainlab and Inomed.

Competing interests

The authors report no competing interests.

Supplementary material

Supplementary material is available at *Brain* online.

References

1. Gibbs FA, Davis H, Lennox WG. The electro-encephalogram in epilepsy and in conditions of impaired consciousness. *Arch NeurPsych*. 1935;34(6):1133–1148.
2. Marsan CA, Zivin LS. Factors related to the occurrence of typical paroxysmal abnormalities in the EEG records of epileptic patients. *Epilepsia*. 1970;11(4):361–381.
3. Sundaram M, Hogan T, Hiscock M, Pillay N. Factors affecting interictal spike discharges in adults with epilepsy. *Electroencephalogr Clin Neurophysiol*. 1990;75(4):358–360.
4. Hufnagel A, Dümpelmann M, Zentner J, Schijns O, Elger CE. Clinical relevance of quantified intracranial interictal spike activity in presurgical evaluation of epilepsy. *Epilepsia*. 2000;41(4):467–478.
5. Kleen JK, Scott RC, Holmes GL, et al. Hippocampal interictal epileptiform activity disrupts cognition in humans. *Neurology*. 2013;81(1):18–24.
6. Reed CM, Mosher CP, Chandravadia N, Chung JM, Mamelak AN, Rutishauser U. Extent of single-neuron activity modulation by hippocampal interictal discharges predicts declarative memory disruption in humans. *J Neurosci*. 2020;40(3):682–693.
7. Karoly PJ, Freestone DR, Boston R, et al. Interictal spikes and epileptic seizures: Their relationship and underlying rhythmicity. *Brain*. 2016;139(Pt 4):1066–1078.
8. Curtis M, Tassi L, Lo Russo G, Mai R, Cossu M, Francione S. Increased discharge threshold after an interictal spike in human focal epilepsy. *Eur J Neurosci*. 2005;22(11):2971–2976.
9. Spencer SS, Goncharova II, Duckrow RB, Novotny EJ, Zaveri HP. Interictal spikes on intracranial recording: Behavior, physiology, and implications. *Epilepsia*. 2008;49(11):1881–1892.
10. Rasmussen T. Characteristics of a pure culture of frontal lobe epilepsy. *Epilepsia*. 1983;24(4):482–493.
11. Jacobs J, Zijlmans M, Zelmann R, et al. High-frequency electroencephalographic oscillations correlate with outcome of epilepsy surgery. *Ann Neurol*. 2010;67(2):209–220.
12. Jacobs J, Wu JY, Perucca P, et al. Removing high-frequency oscillations: A prospective multicenter study on seizure outcome. *Neurology*. 2018;91(11):e1040–e1052.
13. Wu JY, Sankar R, Lerner JT, Matsumoto JH, Vinters HV, Mathern GW. Removing interictal fast ripples on electrocorticography linked with seizure freedom in children. *Neurology*. 2010;75(19):1686–1694.
14. Zijlmans M, Jacobs J, Zelmann R, Dubeau F, Gotman J. High-frequency oscillations mirror disease activity in patients with epilepsy. *Neurology*. 2009;72(11):979–986.
15. Perucca P, Dubeau F, Gotman J. Intracranial electroencephalographic seizure-onset patterns: Effect of underlying pathology. *Brain*. 2014;137(Pt 1):183–196.
16. Schönberger J, Frauscher B, von Ellenrieder N, Avoli M, Dubeau F, Gotman J. Fast ripple analysis in human mesial temporal lobe epilepsy suggests two different seizure-generating mechanisms. *Neurobiol Dis*. 2019;127:374–381.

17. Buzsaki G, Horvath Z, Urioste R, Hetke J, Wise K. High-frequency network oscillation in the hippocampus. *Science*. 1992;256(5059): 1025–1027.
18. Foster DJ, Wilson MA. Reverse replay of behavioural sequences in hippocampal place cells during the awake state. *Nature*. 2006; 440(7084):680–683.
19. Vaz AP, Wittig JH, Inati SK, Zaghloul KA. Replay of cortical spiking sequences during human memory retrieval. *Science*. 2020; 367(6482):1131–1134.
20. Buzsáki G. Two-stage model of memory trace formation: A role for "noisy" brain states. *Neuroscience*. 1989;31(3):551–570.
21. Jacobs J, Kobayashi K, Gotman J. High-frequency changes during interictal spikes detected by time-frequency analysis. *Clin Neurophysiol*. 2011;122(1):32–42.
22. Lachner-Piza D, Jacobs J, Bruder JC, Schulze-Bonhage A, Stieglitz T, Dümpelmann M. Automatic detection of high-frequency-oscillations and their sub-groups co-occurring with interictal-epileptic-spikes. *J Neural Eng*. 2020;17(1):016030.
23. Ren L, Kucewicz MT, Cimbalnik J, et al. Gamma oscillations precede interictal epileptiform spikes in the seizure onset zone. *Neurology*. 2015;84(6):602–608.
24. van KN, Klooster MA, van 'T, Leijten FSS, Jacobs J, Braun KPJ, Zijlmans M. Ripples on rolandic spikes: A marker of epilepsy severity. *Epilepsia*. 2016;57(7):1179–1189.
25. Kramer MA, Ostrowski LM, Song DY, et al. Scalp recorded spike ripples predict seizure risk in childhood epilepsy better than spikes. *Brain*. 2019;142(5):1296–1309.
26. Ylinen A, Bragin A, Nadasdy Z, et al. Sharp wave-associated high-frequency oscillation (200 Hz) in the intact hippocampus: Network and intracellular mechanisms. *J Neurosci*. 1995;15(1 Pt 1):30–46.
27. Klausberger T, Magill PJ, Márton LF, et al. Brain-state- and cell-type-specific firing of hippocampal interneurons in vivo. *Nature*. 2003;421(6925):844–848.
28. Bragin A, Benassi SK, Kheiri F, Engel J. Further evidence that pathologic high-frequency oscillations are bursts of population spikes derived from recordings of identified cells in dentate gyrus. *Epilepsia*. 2011;52(1):45–52.
29. Wyler AR, Ojemann GA, Ward AA. Neurons in human epileptic cortex: Correlation between unit and EEG activity. *Ann Neurol*. 1982;11(3):301–308.
30. Keller CJ, Truccolo W, Gale JT, et al. Heterogeneous neuronal firing patterns during interictal epileptiform discharges in the human cortex. *Brain*. 2010;133(6):1668–1681.
31. Hefft S, Brandt A, Zwick S, et al. Safety of hybrid electrodes for single-neuron recordings in humans. *Neurosurgery*. 2013;73(1): 78–85.
32. Zelmann R, Zijlmans M, Jacobs J, Châtillon C-E, Gotman J. Improving the identification of High Frequency Oscillations. *Clin Neurophysiol*. 2009;120(8):1457–1464.
33. Roehri N, Pizzo F, Bartolomei F, Wendling F, Bénar C-G. What are the assets and weaknesses of HFO detectors? A benchmark framework based on realistic simulations. *Plos One*. 2017;12(4): e0174702.
34. Roehri N, Lina J-M, Mosher JC, Bartolomei F, Bénar C-G. Time-frequency strategies for increasing high-frequency oscillation detectability in intracerebral EEG. *IEEE Trans Biomed Eng*. 2016; 63(12):2595–2606.
35. Chaure FJ, Rey HG, Quian Quiroga R. A novel and fully automatic spike-sorting implementation with variable number of features. *J Neurophysiol*. 2018;120(4):1859–1871.
36. Quiroga RQ, Mukamel R, Isham EA, Malach R, Fried I. Human single-neuron responses at the threshold of conscious recognition. *Proc Natl Acad Sci U S A*. 2008;105(9):3599–3604.
37. Faraut MCM, Carlson AA, Sullivan S, et al. Dataset of human medial temporal lobe single neuron activity during declarative memory encoding and recognition. *Sci Data*. 2018;5(1): 180010.
38. Csicsvari J, Hirase H, Czurko A, Buzsáki G. Reliability and state dependence of pyramidal cell–interneuron synapses in the hippocampus: An ensemble approach in the behaving rat. *Neuron*. 1998;21(1):179–189.
39. Elahian B, Lado NE, Mankin E, et al. Low-voltage fast seizures in humans begin with increased interneuron firing: LVF Onset Seizures. *Ann Neurol*. 2018;84(4):588–600.
40. Oostenveld R, Fries P, Maris E, Schoffelen J-M. FieldTrip: Open source software for advanced analysis of MEG, EEG, and invasive electrophysiological data. *Comput Intell Neurosci*. 2011;2011: 156869.
41. Zhang H, Fell J, Staresina BP, Weber B, Elger CE, Axmacher N. Gamma power reductions accompany stimulus-specific representations of dynamic events. *Curr Biol*. 2015;25(5): 635–640.
42. Winkler AM, Ridgway GR, Webster MA, Smith SM, Nichols TE. Permutation inference for the general linear model. *Neuroimage*. 2014;92:381–397.
43. Alvarado-Rojas C, Lehongre K, Bagdasaryan J, et al. Single-unit activities during epileptic discharges in the human hippocampal formation. *Front Comput Neurosci*. 2013;7:140-
44. van Klink N, Frauscher B, Zijlmans M, Gotman J. Relationships between interictal epileptic spikes and ripples in surface EEG. *Clin Neurophysiol*. 2016;127(1):143–149.
45. Bragin A, Engel J, Wilson CL, Fried I, Mathern GW. Hippocampal and entorhinal cortex high-frequency oscillations (100–500 Hz) in human epileptic brain and in kainic acid-treated rats with chronic seizures. *Epilepsia*. 1999;40(2):127–137.
46. Matsumoto H, Marsan CA. Cortical cellular phenomena in experimental epilepsy: Interictal manifestations. *Exp Neurol*. 1964; 9(4):286–304.
47. Ulbert I, Heit G, Madsen J, Karmos G, Halgren E. Laminar analysis of human neocortical interictal spike generation and propagation: Current source density and multiunit analysis in vivo. *Epilepsia*. 2004;45(Suppl 4):48–56.
48. de Curtis M, Avanzini G. Interictal spikes in focal epileptogenesis. *Progr Neurobiol*. 2001;63(5):541–567.
49. Bonifazi P, Goldin M, Picardo MA, et al. GABAergic hub neurons orchestrate synchrony in developing hippocampal networks. *Science*. 2009;326(5958):1419–1424.
50. Marissal T, Bonifazi P, Picardo MA, et al. Pioneer glutamatergic cells develop into a morpho-functionally distinct population in the juvenile CA3 hippocampus. *Nat Commun*. 2012;3(1):1316-
51. Klausberger T, Somogyi P. Neuronal diversity and temporal dynamics: The unity of hippocampal circuit operations. *Science*. 2008;321(5885):53–57.
52. Foffani G, Uzcategui YG, Gal B, Menendez de la Prida L. Reduced spike-timing reliability correlates with the emergence of fast ripples in the rat epileptic hippocampus. *Neuron*. 2007;55(6): 930–941.
53. Jiruska P, Alvarado-Rojas C, Schevon CA, et al. Update on the mechanisms and roles of high-frequency oscillations in seizures and epileptic disorders. *Epilepsia*. 2017;58(8): 1330–1339.

54. Sabolek HR, Swiercz WB, Lillis KP, et al. A candidate mechanism underlying the variance of interictal spike propagation. *J Neurosci*. 2012;32(9):3009–3021.
55. Muldoon SF, Soltesz I, Cossart R. Spatially clustered neuronal assemblies comprise the microstructure of synchrony in chronically epileptic networks. *PNAS*. 2013;110(9):3567–3572.
56. Staresina BP, Bergmann TO, Bonnefond M, et al. Hierarchical nesting of slow oscillations, spindles and ripples in the human hippocampus during sleep. *Nature Neurosci*. 2015;18(11):1679–1686.
57. Worrell GA, Gardner AB, Stead SM, et al. High-frequency oscillations in human temporal lobe: Simultaneous microwire and clinical macroelectrode recordings. *Brain*. 2008;131(4):928–937.
58. Bragin A, Mody I, Wilson CL, Engel J. Local generation of fast ripples in epileptic brain. *J Neurosci*. 2002;22(5):2012–2021.
59. Juergens E, Guettler A, Eckhorn R. Visual stimulation elicits locked and induced gamma oscillations in monkey intracortical- and EEG-potentials, but not in human EEG. *Exp Brain Res*. 1999;129(2):247–259.
60. Gerstein GL, Clark WA. Simultaneous studies of firing patterns in several neurons. *Science*. 1964;143(3612):1325–1327.
61. Kunz L, Maidenbaum S, Chen D, Wang L, Jacobs J, Axmacher N. Mesoscopic neural representations in spatial navigation. *Trends Cogn Sci*. 2019;23(7):615–630.
62. Sagi V, Evans MS. Relationship between high-frequency oscillations and spikes in a case of temporal lobe epilepsy. *Epilepsy Behav Case Rep*. 2016;6:10–12.